Proceedings of the ASME 2020
International Design Engineering Technical Conferences
and Computers and Information in Engineering Conference
IDETC/CIE2020
August 17-19, 2020, Virtual, Online

DETC2020-22430

STIFFNESS MODULATION FOR A PLANAR MOBILE CABLE-DRIVEN PARALLEL MANIPULATORS VIA STRUCTURAL RECONFIGURATION

Adhiti Raman[1], Matthias Schmid[1], Venkat Krovi[1]

[1]Clemson University, Clemson, SC, United States

ABSTRACT

Mobile Cable-Driven Parallel Manipulators (m-CDPM) are a sub-class of CDPM with greater-capabilities (antagonistic cable-tensioning and reconfigurability) by virtue of mobility of the base-winches. In past work, we had also explored creation of adjustable spring-stiffness modules, in-line with cables, which decouple cable-stiffness and cable-tensions. All these internal-freedoms allow an m-CDPM to track desired trajectories while equilibrating end-effector wrenches and improving lateral disturbance-rejection. However, parameter and configuration selection is key to unlocking these benefits.

To this end, we consider an approach to partition task-execution into a primary (fast) winch-tension control and secondary (slow) reconfiguration and joint-stiffness modulation. This would enable a primary trajectory-tracking task together with secondary task-space stiffness tailoring, using system-reconfiguration and joint-stiffness modulation. In this paper, we limit our scope to feasibility-evaluation to achieve the stiffness modulation as a secondary goal within an offline design-optimization setting (but with an eye towards real-time implementation)

These aspects are illustrated in the context of a 3-PRP m-CDPM for tracking a desired trajectory within its wrench-feasible workspace. The secondary-task is the directional-alignment and shaping of the stiffness ellipsoid to shape the disturbance-rejection characteristics along the trajectory. The optimization is solved through constrained minimization of a multi-objective weighted cost function subject to non-linear workspace feasibility, and inequality stiffness and tension constraints.

Keywords: m-CPDM, Parallel Robotics, Cable Robotics, Structural Reconfiguration, Stiffness modulation

NOMENCLATURE

m	Number of cables
n	Degrees of freedom
l_i	Cable length
$\mathbf{f}$	Tension in the cables
$\mathbf{w}$	Wrench at the end effector
$\mathbf{J}$	velocity Jacobian
$\mathbf{P}$	Pulling map
$\mathbf{K_x}$	Cartesian stiffness matrix
$\mathbf{K_s}$	Joint stiffness matrix
e_t	Tangent to trajectory
e_n	Normal to trajectory
$\mathbf{a}$	Vector of design variables
G	Non-analytic cost function
C	Stiffness isotropicity
λ	Eigenvalues of $\mathbf{K_x}$

1. INTRODUCTION

Cable driven parallel manipulators (CDPMs) are a class of closed kinematic chain robots where the end effector is tensioned by multiple flexible cables. CPDMs feature a moving end-effector platform driven by a set of parallel actively winched cables (or tendons, or wires). The coordinated spooling and tensioning of the cables now permits control of the position and orientation of the moving platform [1].

Compared to rigid link parallel-manipulators, CDPMs have a larger payload weight to actuation power ratio, smaller system weight and inertia, and depending on the design, can have larger reachable workspace and manipulation flexibility – with a requirement of redundant $(n+1)$ active cables due to the unilateral cable-tension constraints. Compared to rigid link

robots, the flexibility offered from cable routing and actuation location allows reduced total moving mass/inertia and better dynamic performance over potentially larger workspaces leading to their deployment in many large-scale material handling applications.

Mobile-CDPMs are a subclass of CDPMs where the addition of base mobility now offers greater flexibility [2, 3, 4] by virtue of added kinematic and actuation redundancy and ability to tailor the internal configuration to suit the task at hand. As with all parallel-manipulators, performance of the system is critically-dependent upon selection of: (i) the architecture (individual or in-parallel cable-architecture, number of cables, attachment of cables to fixed or moving platforms); (ii) various dimensional characteristics (size, shape, size of motors); and (iii) ultimately on selection of the optimum configuration exploiting the internal degrees-of-freedom. Even in traditional CDPMs, the natural $n+1$ cable requirement for fully restraining an n DOF end-effector can be exploited to satisfy primary goals, such as tracking a trajectory of interest [5], as well as secondary desirable criterions such as, selecting the optimum cable tension [6, 7], maintaining a certain manipulability [8, 9] or stiffness configuration over that trajectory [10]. Redundancy-resolution is critical for control. This is more valid for mobile CDPMs – as it offers even greater opportunity to satisfy secondary criteria. For example, the additional actuation parameters can reduce the overall load requirements on individual actuators by distributing the forces more evenly [11]. Active switched-selection of the set of actuated joints within the closed kinematic-chain offers another opportunity for design selection.

Performance characterization (in terms of performance-metrics tied to various critical parameters) is key to systematically unlocking the opportunities within optimization-based configuration-planning framework. The recent work by Jaquier et al. [9] used internal posture-reconfigurability of a redundant serial chain robot to match a desired manipulability ellipsoid as a secondary objective of a trajectory tracking task proving the continuing relevancy of such approaches. In a similar vein, exploiting the force/velocity duality, we seek to modulate the stiffness ellipsoids within our mobile CDPMs to improve disturbance rejection at the end effector during trajectory tracking.

1.1 Structural Reconfiguration

The base-winch location selection has a critical impact on the workspace (both size/quality) for CDPMs. Actuated base mobility in traditional $n-DOF$ fully constrained cable robot configurations with $n+1$ cables increases the overall kinematic- and actuation-redundancy and can allow for a slower configuration-shaping together with cable-tension control.

Hence, in lieu of a one-time design-optimization for base-winch locations for global workspace quality, we explore exploiting base-winch mobility for localized workspace quality enhancements (e.g. enhanced stiffness-rejection in certain directions) at various points along the trajectory. In our past work, the redundancy in configuration in mobile-CDPMs was exploited to redistribute the internal tensions within the cables as well as modulate the stiffness [10]. We had also explored decoupling cable-tension and cable-stiffness with adjustable spring-stiffness modules, in-line with cables [12]. Combinedly, these offer an opportunity for task-space stiffness-modulation by coordinating: (i) joint-stiffness; (ii) antagonistic cable-tensions; and (iii) system-reconfiguration.

Specifically, instead of a fast/active antagonistic tension modulation, there is now an opportunity to utilize a slower structural reconfiguration (offered by base-winches) to improve task-space stiffness. This paper builds on these efforts for evaluating feasibility of such an approach for a 3-PRP planar mobile CDPM (shown in Figure 1). Pre-determined trajectory/load profiles are assumed. Actuator-profile planning is performed (in a non-real-time/offline setting) for establishing the fundamental viability of trajectory tracking while also aligning the principal axis of the stiffness ellipsoid to be normal to the end-effector tangent-velocity direction for lateral disturbance rejection.

2. MATHEMATICAL MODEL

2.1 Kinetostatics

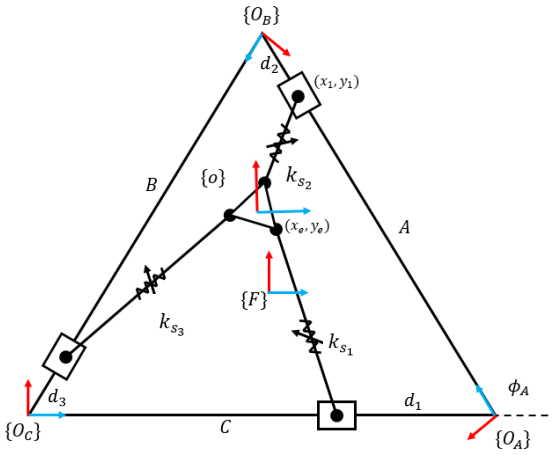

FIGURE 1: PARAMETERS FOR A 3-PRP PLANAR MOBILE CABLE DRIVEN PARALLEL MANIPULATOR

Illustrated in Fig. 1 are the key parameters for a 3-PRP mobile CDPM with a rigid body end-effector of known dimensions. Based on the modelling in [12], we add springs inline to the cables and assume them to be adjustable spring-stiffness modules (k_{s_i}) that also decouple the tension/stiffness in the cable. Given slider positions (d_i) and end-effector wrenches at any given point of time, a kinetostatic model can be formulated directly from equations of static-equilibrium. However, in pursuing a more general approach, we build upon the Lie group based formulation in Zhou et al. [13] to determine the tension $\mathbf{f}$ in the cables:

$$-[\mathbf{J}^{\mathbf{T}}]_{n\times m}[\mathbf{f}]_{m\times 1} = [\mathbf{w}]_{n\times 1} \quad (1)$$

where $\mathbf{w}$ denotes the external wrench and $-[\mathbf{J^T}]$ is the force Jacobian, henceforth known as the pulling map, $\mathbf{P}$. Assuming the end-effector pose is known (from the trajectory), the pulling map, $\mathbf{P}$, is entirely dependent on the static and variable configuration parameters. Following the derivation of the pulling map in [13] each column of the pulling map is the cable wrench basis direction and is expressed in the end-effector frame $\{o\}$ as,

$$ {}^{o}P_i = \begin{bmatrix} -\cos(\gamma_i) \\ \sin(\gamma_i) \\ y_{oc_i}\cos(\gamma_i) + x_{oc_i}\sin(\gamma_i) \end{bmatrix} \tag{2} $$

where γ_i is the angle between direction of cable tension, f_i, and the x-axis of frame $\{o\}$. Let x_{oc_i} and y_{oc_i} be the x and y coordinates of the contact point of the cable on the end effector frame. $\mathbf{P}$ is then extracted by concatenating the wrench basis.

$$ \mathbf{P} = \begin{bmatrix} | & | & | & | \\ {}^{o}P_1 & {}^{o}P_2 & \dots & {}^{o}P_m \\ | & | & | & | \end{bmatrix} \tag{3} $$

For $m = 3$ and $n = 2$ the pulling map is given by

$$ \mathbf{P} = \begin{bmatrix} \frac{x_{oc_1}-x_1}{||l_1||} & \frac{x_{oc_2}-x_2}{||l_2||} & \frac{x_{oc_3}-x_3}{||l_3||} \\ \frac{y_{oc_1}-y_1}{||l_1||} & \frac{y_{oc_2}-y_2}{||l_2||} & \frac{y_{oc_3}-y_3}{||l_3||} \end{bmatrix} \tag{4} $$

$$ \forall \, ||l_i|| = (x_i - x_{oc_i})^2 + (y_i - y_{oc_i})^2 $$

An expression for the particular- and homogenous-components of the cable-tensions can then be obtained using the pseudo-inverse $\mathbf{P}^{\#}$ as:

$$ \mathbf{f} = -\mathbf{P}^{\#}\mathbf{w} + (\mathbf{I} - \mathbf{P}^{\#}\mathbf{P})\boldsymbol{\alpha} \tag{5} $$

where α is any arbitrary vector which when filtered through the null space can ensure that $\mathbf{f}$ is always positive to ensure force closure.

2.2 Stiffness Matrix

The Cartesian stiffness matrix is derived in [5] to be:

$$ \mathbf{K_x} = -\left[\frac{\partial \mathbf{P}}{\partial x_e}, \frac{\partial \mathbf{P}}{\partial y_e}, \frac{\partial \mathbf{P}}{\partial \phi_e}\right]\mathbf{f} + \mathbf{P}\mathbf{K_s}\mathbf{P^T} \tag{6} $$

where x_e, y_e and ϕ_e are the coordinates of the end effector in frame $\{F\}$, and $\mathbf{K_s}$ is the joint space stiffness – a diagonal matrix composed of individual cable stiffnesses k_i.

$$ \mathbf{K_x} = -\mathbf{H}\mathbf{f} + \mathbf{P}\mathbf{K_s}\mathbf{P^T} \tag{7} $$

$$ \mathbf{K_x} = \mathbf{K_g} + \mathbf{K_c} \tag{8} $$

where $\mathbf{K_x}$ is the Cartesian or task space stiffness and $\mathbf{H}$ is a Hessian tensor. As noted by Behzadipour *et al.* [14] the first term $\mathbf{K_g}$ represents the Cartesian stiffness contribution depending on the configuration (varying direction) and cable pre-tension (magnitude). The second term $\mathbf{K_c}$ represents the Cartesian stiffness contribution from elastic-cable stiffnesses in $\mathbf{K_s}$ while the configuration (direction) and tensions (magnitude) are held constant. The three mechanisms to modulate $\mathbf{K_x}$ arise from ability to: (i) control antagonistic-components of internal tension $\mathbf{f}$ (exploiting actuation redundancy) [5]; (ii) modulate cable joint space stiffness $\mathbf{K_s}$, [10] and/or (iii) alter the configuration-dependent pulling map $\mathbf{P}$ [10]. In this paper, we focus on building towards an optimization-based framework for the adaptation of $\mathbf{K_s}$ and $\mathbf{P}$. We do so by setting up an optimization problem with appropriate selection of the objective functions and constraints that depend on the stiffness ellipse.

2.3 Optimization Objective Function

The objective function is selected as a unit weighted blend of two non-dimensionalized objective functions, by an appropriate selection of the weight, $0 \leq W \leq 1$.

$$ G = W(u_{s1}.e_t)^2 + (1 - W)\frac{\lambda_{min}}{\lambda_{max}} \tag{9} $$

where the first term corresponds to the orientation of the ellipse and the second term corresponds to shape manipulation which are explained below.

Orienting the stiffness ellipse: Our primary objective function is to align the task-space Cartesian stiffness ellipse $\mathbf{K_x}$ to the normal to the tangent of the trajectory at that time instant and manipulating the shape of the ellipsoid to reject only motion that is lateral to the direction of motion.

$$ Obj_1 = (u_{s_1}.e_t)^2 \tag{10} $$

where u_{s_1} is the principal eigenvector associated with the largest eigenvalue of $\mathbf{K_x}$, corresponding to the major axis of the ellipse, e_t is the unit tangent vector along the trajectory at any point.

Stiffness Isotropicity: There is an opportunity to consider an additional component within the optimization objective function. Much like the Jacobian-based manipulability ellipsoid (and derivative measures), the stiffness ellipsoid (and derivative isotropicity measure) captures the ability of equilibration (active- and structural) to resist external disturbances in all directions. For directional resistance, controlling the value of the stiffness isotropicity allows control of the shape of the ellipsoid.

The stiffness isotropicity is given by:

$$ Obj_2 = C = \frac{\lambda_{min}}{\lambda_{max}};\ 0 < C < 1 \tag{11} $$

where λ_{max} and λ_{min} are maximum and minimum eigenvalues of $\mathbf{K_x}$.

Role of selection of W: Setting W=1 in Eq. 9 essentially selects the first objective function. Minimizing the weighted objective now helps to align the major axis to be orthogonal to the direction of motion, but control over the shape is relinquished. Performing optimization with lower values of W permits tailoring of both the orientation of the ellipse as well as the overall shape. In what follows, we will present results only for the case W=0.8. However, a pareto frontier evaluation could be used to determine the most suitable value of W.

2.4 Optimization Implementation

The primary criteria for feasibility (necessary condition) is wrench closure where the wrench feasibility is maintained by biasing the solution towards positive tensions in the cables. To chart a trajectory, the optimization scheme must be part of a closed loop control problem [15].

Due to redundancy, $[\mathbf{P}]_{n\times m}$ is a non-square matrix with $n < m$ which would map the wrench forces to infinitely many solutions. The resulting tensions in the cable must always be positive, necessitating a feasibility check at the start of the procedure. A primary step determines $\boldsymbol{\alpha}$ in equation (4), such that the tension in the cables $\mathbf{f}_{m\times 1}$ is greater than or equal to a lower-bound tension value, f_{min}.

The adjustable stiffness modules [12] permit decoupling of cable-tension and cable-stiffness and thus it is possible for it to have any arbitrary positive value without affecting the desired joint stiffness. By setting an arbitrary continuous external wrench on the end effector, the internal tension is then dependent only on the base configuration. The change in cable lengths is given by the forward velocity kinematics as:

$$\dot{\mathbf{l}} = \mathbf{P}^{\mathbf{T}}\dot{\mathbf{x}} \tag{12}$$

where $\dot{\mathbf{x}}$ is known from the trajectory specification.

Three potential cases can be considered: (i) changing only the joint stiffnesses; (ii) changing only the winch-base locations; and (iii) combining the two.

Case 1: Changing only the spring stiffnesses, $\mathbf{K_s}$: Given known base locations and end effector location at a time instant and a nominal external wrench the following optimization problem can be developed with changing values of $\mathbf{K_s}$ as the design-variables.

$$\min_{k_{s_i}} G(\mathbf{K_s}) = W(u_{s1}.e_t)^2 + (1-W)\frac{\lambda_{min}}{\lambda_{max}}$$

$$subject\ to: \quad \mathbf{K_x} = \frac{\partial \mathbf{P}}{\partial \mathbf{x}}\mathbf{f} + \mathbf{P}\mathbf{K_s}\mathbf{P}^{\mathbf{T}}$$

$$0 \le k_{s_i} \le k_{max} \ \forall\, i \in \{0, m\}$$

$$f_i > f_{min} \ \forall\, i \in \{0, m\}$$

The weighted blend of two objectives discussed in equation (9) is examined for W=0.8.

Case 2: Changing only base-winch locations ($\mathbf{d_i}$): Given an external wrench, constant values for k_{s_i}, and an end effector location at a time instant, a similar optimization problem can be formulated – this time with changing base-winch locations as the design-variables

$$\min_{d_i} G(\mathbf{d}) = W(u_{s1}.e_t)^2 + (1-W)\frac{\lambda_{min}}{\lambda_{max}},$$

$$subject\ to: \quad \mathbf{K_x} = \frac{\partial \mathbf{P}}{\partial \mathbf{x}}\mathbf{f} + \mathbf{P}\mathbf{K_s}\mathbf{P}^{\mathbf{T}}$$

$$0 \le d_i \le d_{max} \ \forall\, i \in \{0, m\}$$

$$f_i > f_{min} \ \forall\, i \in \{0, m\}$$

It is noteworthy that changing the base-winch positions affects the wrench-closure workspace. Hence, an additional check needs to be performed to ensure that any given trajectory point continues to lie within the wrench feasible workspace of the modulated configuration. This check is set as a non-linear inequality constraint within the optimization algorithm.

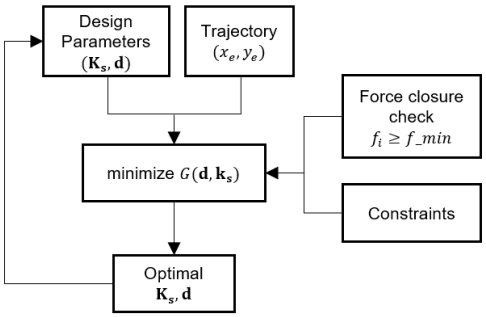

FIGURE 2: OPTIMIZATION PROCESS FLOW

Case 3: Changing both base-winch locations $\mathbf{d}$ and $\mathbf{K_s}$: Finally, we perform an optimization using both k_{s_i} and d_i simultaneously given an external wrench and end effector location at any time instant.

$$\min_{k_{s_i}, d_i} G(\mathbf{K_s}, \mathbf{d}) = W(u_{s1}.e_t)^2 + (1-W)\frac{\lambda_{min}}{\lambda_{max}},$$

$$subject\ to: \quad \mathbf{K_x} = \frac{\partial \mathbf{P}}{\partial \mathbf{x}}\mathbf{f} + \mathbf{P}\mathbf{K_s}\mathbf{P}^{\mathbf{T}}$$

$$0 \le k_{s_i} \le 10 \ \forall\, i \in \{0, m\}$$

$$0 \le d_i \le d_{max} \ \forall\, i \in \{0, m\}$$

$$f_i > f_{min} \ \forall\, i \in \{0, m\}$$

where the gradient descent minimization is applied on the vector of all considered actuators, $\mathbf{a} = \{\mathbf{d}, \mathbf{K_s}\}$

$$a_{i_{t+1}} = a_{i_t} - \eta \frac{\partial G(\mathbf{d}, \mathbf{K_s})}{\partial a_i} \quad (13)$$

Again, as in Case 2, an additional check needs to be performed to ensure that any given trajectory point continues to lie within the wrench feasible workspace of the modulated configuration.

Fig 2. shows a process flow diagram to summarize the optimization process.

3 RESULTS AND DISCUSSION

The optimization is applied to the specific case of a 3-PRP m-CDPM design, where m = 3, and n = 2. The chosen trajectory is a sinusoid and direction of the constant magnitude wrench vector is dependent on the direction of motion.

3.1 Benchmark model – d and K_s are fixed

When the position and stiffness are arbitrarily chosen to have constant values, then the problem mimics the case of a standard planar 3-cable structure. The stiffness ellipsoid, and consequently the manipulability ellipsoid will have no direction constraint. The end-effector is non-stiff and has the inability to reject disturbances in most directions.

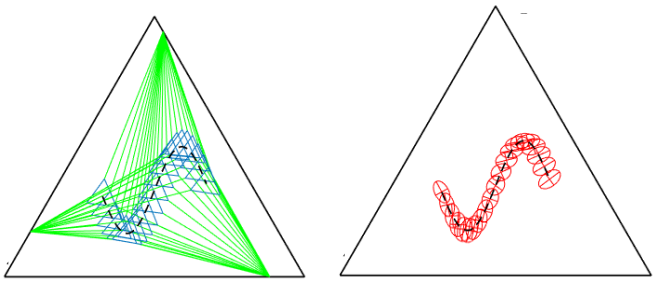

(a) (b)

FIGURE 3: FIXED WINCH POSITIONS AND CONSTANT SPRING STIFFNESSES (A) VARIOUS CONFGURATIONS OVER TRAJECTORY (B) STIFFNESS ELLIPSES OVER TRAJECTORY

3.2 Case 1: Changing only K_s

For the first case, where the bases are fixed, the resulting optimized configuration are shown below in Figure 4(a) while the stiffness ellipsoid alignment is shown in Figure 4(b).

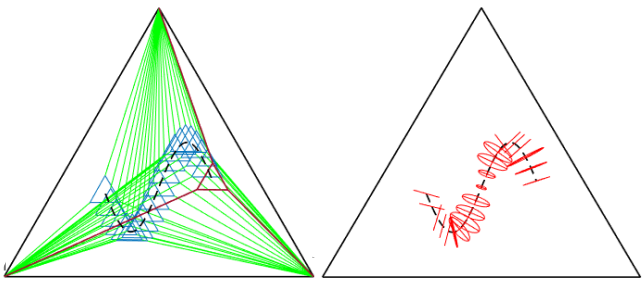

(a) (b)

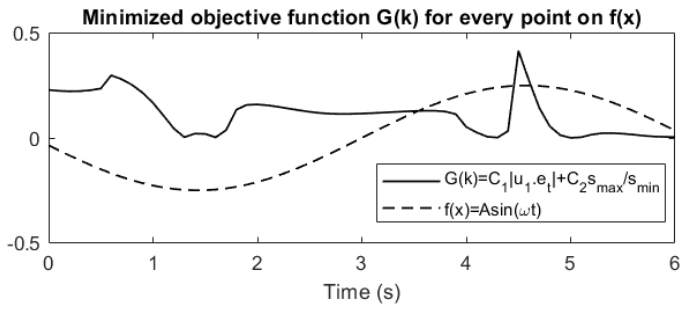

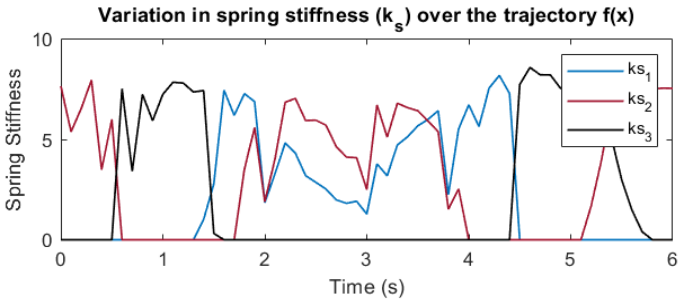

(c)

FIGURE 4: FIXED WINCH POSITION AND VARIED JOINT STIFFNESS: (A) VARIOUS CONFIGURATIONS FOR $W = 0.8$; (B) STIFFNESS ELLIPSES ALONG TRAJECTORY; AND (C) COST FUNCTION, TRAJECTORY AND $\mathbf{k_s}$ vs TIME

We note that stiffness ellipses are aligned with the major axis perpendicular to the tangent of the trajectory i.e. improved disturbance rejection on the normal to the trajectory. Figure 4(c) shows the minimized cost function $G(k_{s_i})$ for every point on the trajectory and the variation in k_1, k_2 and k_3 along the span of this trajectory. At certain configurations, the resulting orientation and shape is sub-optimal. This can be resolved by exploiting the redundancy in winch position.

3.3 Case 2: Changing only d

In this case, the base winch locations are subject to optimization while the spring stiffnesses are maintained at a constant value. All other parameters remain the same.

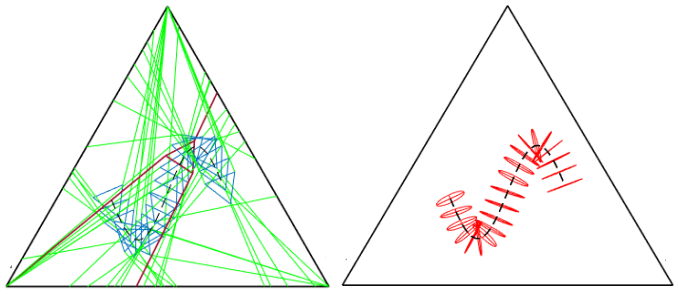

(a) (b)

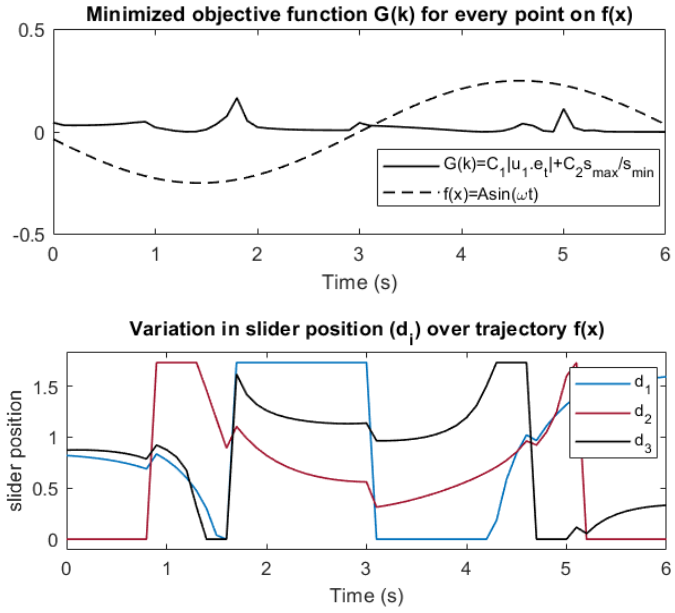

(c)

FIGURE 5: VARIED WINCH POSITION AND FIXED JOINT STIFFNESS: (A) VARIOUS CONFIGURATIONS FOR $W = 0.8$; (B) STIFFNESS ELLIPSES ALONG TRAJECTORY; AND (C) COST FUNCTION, TRAJECTORY AND $\mathbf{d_i}$ vs TIME

Figure 4(c) shows the minimized cost function $G(d_i)$ for every point on the trajectory and how the winch positions d_1, d_2 and $d_3$change to accommodate this. The jumps in winch position would not be suitable for a real-world implementation and resolving this is beyond the scope of this paper.

3.4 Case 3: Changing both K_s and d

By being able to modulate all six variables, we arrive at a solution that is stiff only in the direction on motion.

Figure 6(c) shows the minimized cost function $G(\mathbf{d}, \mathbf{k_s})$ and the variation in winch positions d_1, d_2, d_3 and stiffnesses k_1, k_2 and k_3 along the span of this trajectory. We note that the optimization can be improved by adding velocity level constraints on the winch movement and stiffness modulation to prevent the abrupt changes.

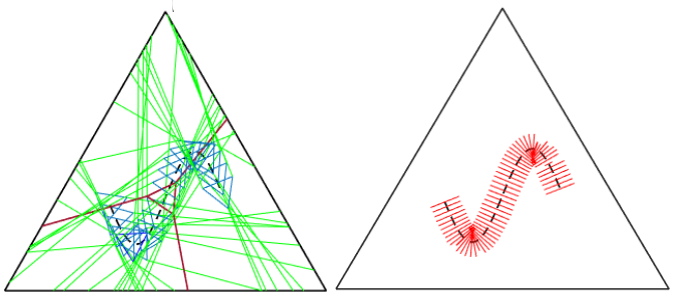

(a) (b)

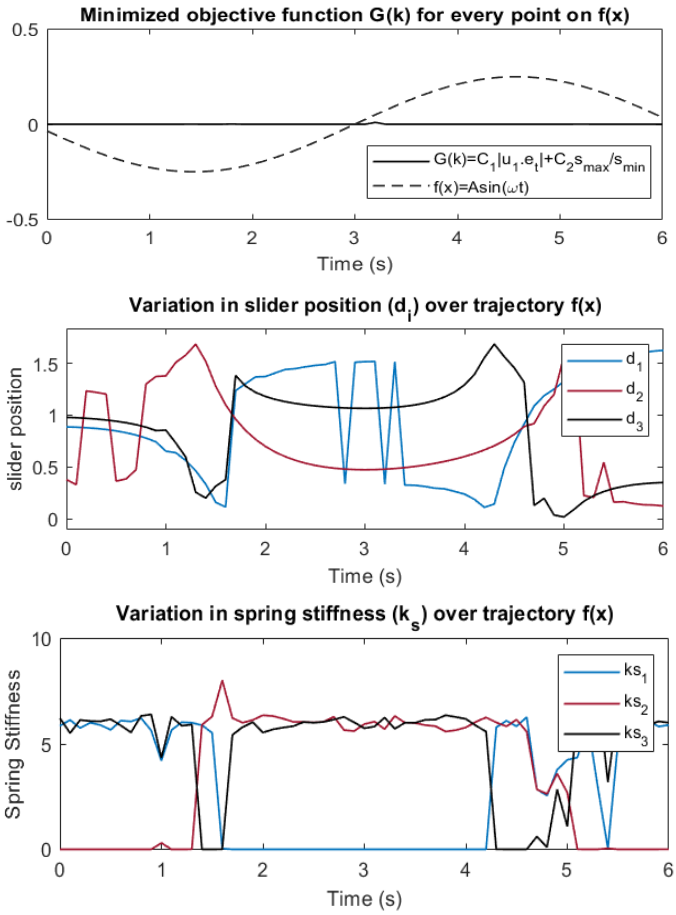

(c)

FIGURE 6: MOVING WINCH POSITIONS AND VARIED JOINT STIFFNESS: (A) VARIOUS CONFIGURATIONS; (B) STIFFNESS ELLIPSES ALONG TRAJECTORY; AND (C) COST FUNCTION AND WINCH POSITIONS $\mathbf{d_i}$ AND STIFFNESS $\mathbf{k_s}$ vs TIME

3. CONCLUSION

Mobile-CDPMs feature significant latent potential to simultaneously track desired trajectories equilibrating any imposed end-effector wrenches while also permitting natural disturbance-rejection. In this paper, we explored the feasibility of 3-PRP m-CDPM to achieve stiffness modulation to enhance disturbance-rejection as a secondary goal to the primary trajectory tracking task within its wrench-feasible workspace. Task-space stiffness modulation is achievable by coordinating: (i) joint-stiffness; (ii) net-zero antagonistic cable-tensions; and (iii) system-configuration. However, parameter- and configuration-selection within a kinematic- and actuation-redundancy resolution framework is key to realizing these benefits. The optimization-based planning effort (for base-winch reconfiguration and joint stiffness adjustments) establishes the initial viability of the approach – however, further work is necessary to improve continuity of the parameter- and

configuration-changes in preparation for experimental validation.

ACKNOWLEDGEMENTS

The authors would like to acknowledge support of their colleagues from ARMLab at the Clemson University International Center for Automotive Research. We also acknowledge partial support for this work from the National Science Foundation via the National Robotics Initiative grant (CMMI- 1924721).

REFERENCES

[1] A. Pott, *Cable-driven parallel robots: theory and application*. Springer, 2018.

[2] M. Anson, A. Alamdari, and V. Krovi, "Orientation workspace and stiffness optimization of cable-driven parallel manipulators with base mobility," *Journal of Mechanisms and Robotics,* vol. 9, no. 3, 2017.

[3] L. Gagliardini, S. Caro, M. Gouttefarde, and A. Girin, "Discrete reconfiguration planning for cable-driven parallel robots," *Mechanism and Machine Theory,* vol. 100, pp. 313-337, 2016.

[4] D. Q. Nguyen and M. Gouttefarde, "Study of reconfigurable suspended cable-driven parallel robots for airplane maintenance," in *2014 IEEE/RSJ International Conference on Intelligent Robots and Systems*, 2014: IEEE, pp. 1682-1689.

[5] K. Yu, L.-F. Lee, C. P. Tang, and V. N. Krovi, "Enhanced trajectory tracking control with active lower bounded stiffness control for cable robot," in *2010 IEEE International Conference on Robotics and Automation*, 2010: IEEE, pp. 669-674.

[6] L. Mikelsons, T. Bruckmann, M. Hiller, and D. Schramm, "A real-time capable force calculation algorithm for redundant tendon-based parallel manipulators," in *2008 IEEE International Conference on Robotics and Automation*, 2008: IEEE, pp. 3869-3874.

[7] S.-R. Oh and S. K. Agrawal, "Cable suspended planar robots with redundant cables: Controllers with positive tensions," *IEEE Transactions on Robotics,* vol. 21, no. 3, pp. 457-465, 2005.

[8] M. Agahi and L. Notash, "Redundancy resolution of wire-actuated parallel manipulators," *Transactions of the Canadian Society for Mechanical Engineering,* vol. 33, no. 4, pp. 561-573, 2009.

[9] N. Jaquier, L. D. Rozo, D. G. Caldwell, and S. Calinon, "Geometry-aware Tracking of Manipulability Ellipsoids," in *Robotics: Science and Systems*, 2018, no. CONF.

[10] X. Zhou, S.-k. Jun, and V. Krovi, "Stiffness modulation exploiting configuration redundancy in mobile cable robots," in *2014 IEEE International Conference on Robotics and Automation (ICRA)*, 2014: IEEE, pp. 5934-5939.

[11] X. Zhou, S.-k. Jun, and V. Krovi, "Tension distribution shaping via reconfigurable attachment in planar mobile cable robots," *Robotica,* vol. 32, no. 2, pp. 245-256, 2014.

[12] X. Zhou, S.-k. Jun, and V. Krovi, "A cable based active variable stiffness module with decoupled tension," *Journal of Mechanisms and Robotics,* vol. 7, no. 1, 2015.

[13] X. Zhou, C. P. Tang, and V. Krovi, "Cooperating mobile cable robots: Screw theoretic analysis," in *Redundancy in Robot Manipulators and Multi-Robot Systems*: Springer, 2013, pp. 109-123.

[14] S. Behzadipour and A. Khajepour, "Stiffness of cable-based parallel manipulators with application to stability analysis," 2006.

[15] H. D. Taghirad and Y. B. Bedoustani, "An analytic-iterative redundancy resolution scheme for cable-driven redundant parallel manipulators," *IEEE Transactions on Robotics,* vol. 27, no. 6, pp. 1137-1143, 2011.